A Comparison of Theoretical, Simulated, and Experimental Results Concerning the Stability of Sigma Delta Modulators

Georgi Tsenov[1], Valeri Mladenov[1], and Joshua D. Reiss[2]

[1] Dept of Theoretical Electrical Engineering, Technical University of Sofia, 8, Kliment Ohridski St., Sofia, Bulgaria
gogotzenov@tu-sofia.bg

[2] Dept of Electronic Engineering, Queen Mary, University of London, Mile End Road, London, E1 4NS
josh.reiss@elec.qmul.ac.uk

ABSTRACT

Sigma delta modulation is a popular form of audio analogue-to-digital and digital-to-analogue conversion, but suffers from stability problems for many designs and many input signals. A general theory of stability in sigma delta modulators has been developed which predicts the stability of a high order one bit sigma delta modulator (SDM) under a variety of designs. In this paper, the theoretical approach to stability as it applies to boundedness of states is explained. Several low pass SDM designs are developed which are intended for audio analogue to digital conversion, and predicted results for stability of these designs are given. Stability is examined both in terms of the maximum allowable DC input amplitude and the theoretical sufficient conditions for stable behavior. Theoretical results are compared with simulated results, and where possible, with experimental results from a realisation of a third order SDM with adjustable parameters. Practical observations are then made concerning the effect of noiseshaping, pole/zero placement, and cut-off frequency on the stability.

1.   INTRODUCTION

Sigma delta modulation is one of the most popular methods for analog to digital (and digital to analog) conversion for audio applications. Yet despite the widespread use of sigma delta modulators (SDMs), a satisfactory theory of their stability is still lacking. In its simplest form, this implies that in general, the maximum allowable input signal which can produce stable behavior for a given design cannot be easily derived.

There has been much research into stability issues in SDMs, but many essential questions remain unsolved. It is fairly easy to show the stability limits of the first

order SDM, but for the standard second order SDM, proof of boundedness is not trivial. A linear programming approach is used by Farrell and Feely[1]. They assumed that there have been some number n^- iterations with negative output. From this, they identify the maximum values of the state space variables for the first positive output bit. This value is used to identify the maximum number of positive output bits which results, n^+. They then find the maximum number of negative output bits which result from the n^+ positive bits. This new value of n^- is strictly less than n^+ and hence the oscillations are bounded. This successfully finds the bounds on the second order SDM and may be extended to second order SDMs with leaky or chaotic integrators and their results bear strong agreement with simulation.

To the best of our knowledge, there is no generally accepted, successful analytical approach to stability in high order SDMs (order greater than 2). Risbo[2] discussed stability of SDMs in detail, primarily from a nonlinear dynamics perspective. But, with the exception of first order SDMs, he did not attempt a method for its determination. A computational approach to finding the invariant sets, which consist of initial conditions giving rise to stable behavior, is derived by Schreier[3-5]. Although neither analytical nor rigorous, it is significant because source code is available, and because results are provided which may be confirmed or denied by other methods. Hein and Zakhor's approach[6] is to use the limit cycles as a measure of stability. Their method is not rigorous in that it postulates that the limit cycles have a convergent bound on the state space variables, and that this is also the bound for non-limit cycle behaviour. Wang[7] converted a third order modulator to a continuous time system by looking at the vector field equations. By considering only boundary points, he is able to convert the 3 dimensional flow into a 2 dimensional return map. Fixed points of this map then yield insight into stability of the SDM. Zhang[8, 9] used a model of the quantizer to estimate stability of a third order SDM. The linearization implies that important phenomena have been omitted. Furthermore, there is little comparison of their results with simulation. Another work by Zhang[10] bears a strong resemblance to the linear programming approach of Feely.

One promising approach is based on representing the sigma delta modulator's loop transfer function as a parallel decomposition of first order filters. Using this decomposition, an Nth order SDM may be considered to be comprised of N first order modulators which interact

only through the quantizer. The stability condition of the system is then determined by the stability conditions of each of the first order modulators but shifted with respect to the origin of the quantizer function. Significantly, this theory does not involve approximating the quantiser as an additive noise source and hence suffers none of the drawbacks of the linear model.

The benefits of using parallel decomposition for analysis of SDMs was first realized in seminal work by Steiner and Yang, but at that time presented only as a framework for understanding stability behavior in low order designs[11], or as a general framework for analysis of high order designs[12]. It was later extended by Mladenov, et al [13, 14] in order to provide exact formulas for stability of certain hypothetical high order designs. The work presented herein further extends and validates this approach by providing concrete results concerning the stability of realistic high order designs that may be applied to audio A/D conversion.

In this paper, the theory given in [13, 14] is applied to both designs described in the literature, and to new high order designs based on standard filter design techniques such as Butterworth, Chebyshev, and iteration/optimization techniques. These designs were chosen such that they will yield performance, particularly in terms of the Signal to Noise ratio, suitable for use as an analog-to-digital converter to be applied to audio signals. These techniques are used to generate low pass filter coefficients for the signal transfer function (or alternatively, high pass filter coefficients for the noise transfer function). Then, the loop filter is found using $G(z) = (1/\mathrm{NTF}(z))-1$. A partial fraction expansion is then applied so that the loop filter may be implemented in parallel form and the theoretical analysis mentioned above can be applied.

The theoretical stability of these designs is then compared with simulated results. An experimental third order SDM with adjustable coefficients was also constructed. The design employed variable resistors which allow all coefficients within the design to be modified. This experimental design showed good agreement with both a PSpice model of the circuitry and the Matlab simulations of the logic level implementation.

The level of DC input at which the SDM goes unstable is reported and compared for theoretical and simulated

systems. The effect of pole/zero placement, filter cut-off frequency, and general noiseshaping characteristics on stability is also discussed. Initial results confirm the existing theory, and discrepancies may be accounted for in part by the fact that current theory provides sufficient, but not necessary, conditions for stable behavior.

2. THEORY

For better understanding, in this chapter we will briefly present the theoretical results given in [13-16]. This theory provides a technique by which the stability of an SDM may be found based on the placement of the poles where the loop filter is represented in parallel canonical form. In Section 2.1, we describe the parallel decomposition. We then describe how the stability of each of the first order sections in the decomposition may be found in Section 2.2. Section 2.3 shows how this may then be used to determine the stability of an arbitrary order SDM with real poles, and in Section 2.4, this is extended to high order SDMs where we consider one complex conjugate pole pair in the loop filter. It should be noted that not all cases have been fully developed. The stability of real poles equal to one, more than one pair of complex poles inside the unit circle, or any number of complex poles on or outside the unit circle, remain an area of active research.

2.1. Parallel Decomposition Of Sigma Delta Modulators

The structure of a basic SDM is shown in Figure 1, and consists of a filter with transfer function $G(z)$ followed by a one-bit quantizer in a feedback loop. The system operates in discrete time.
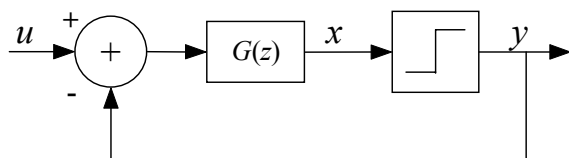

Figure 1. Basic structure of the sigma delta modulator.

The input to the loop is a discrete-time sequence $u(n) \in [-1, 1]$, which is to appear in quantized form at the output. The discrete-time sequence $x(n)$ is the output of the filter and the input to the quantizer. Clearly a single-bit quantizer, which gives an output of $+1$ when its input is positive and -1 when its input is negative, will not provide a good approximation to its input signal. In

other words the quantization noise will be large. This is the reason for the use of the feedback loop, which acts in such a way as to shift this quantization noise away from a certain frequency band. If an input signal from within this frequency band is applied to the loop, most of the noise imposed by the quantization process will lie outside the frequency band of interest and can subsequently be filtered out, leaving a good approximation to the input signal.

Let us consider a Nth order modulator with a loop filter with a transfer function in the form

$$G(z) = \frac{a_1 z^{-1} + ... + a_N z^{-N}}{1 + d_1 z^{-1} + d_2 z^{-2} + ... + d_N z^{-N}} \qquad (1)$$

Suppose the transfer function has N real distinct roots of the denominator. Then using partial fraction expansion we get

$$G(z) = \frac{a_1 z^{-1} + ... + a_N z^{-N}}{(1 - \lambda_1 z^{-1})...(1 - \lambda_N z^{-1})}$$
$$= \frac{b_1 z^{-1}}{1 - \lambda_1 z^{-1}} + ... + \frac{b_N z^{-1}}{1 - \lambda_N z^{-1}} \qquad (2)$$

where the coefficients b_i, $i=1,2,...,N$ of the fractional components can be found easily using the well known formula $b_i = \frac{(1 - \lambda_i z^{-1})}{z^{-1}} G(z)\Big|_{z=\lambda_i}$.

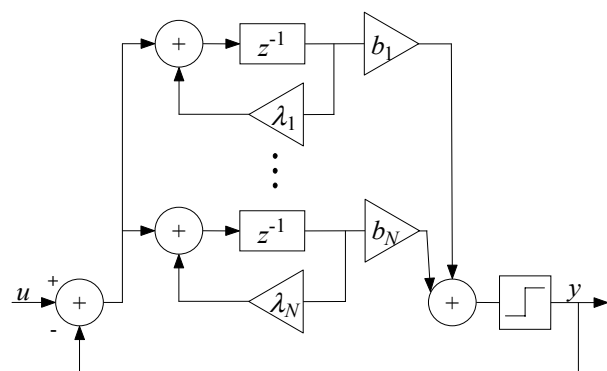The corresponding block diagram of the modulator is given in Figure 2.

Figure 2. Block diagram of the modulator using parallel form of the loop filter.

Based on this presentation the state equations of the SDM are

$$x_k(n+1) = \lambda_k x_k(n) + u(n) - \text{sgn}[\sum_{i=1}^{N} b_i x_i(n)] =$$

$$= \lambda_k x_k(n) + u(n) - \text{sgn}[b_k x_k(n) + \sum_{\substack{i=1 \\ i \neq k}}^{N} b_i x_i(n)], \qquad (3)$$

$$k = 1, 2, ..., N$$

where $\lambda_1, \lambda_2 ..., \lambda_N$ are poles (or modes) of the loop filter and the quantizer function is a sign function

$$\text{sgn}(x) = \begin{cases} 1, & x \geq 0 \\ -1, & x < 0 \end{cases}$$

A brief overview of the results for the stability of first order SDM described by

$$x(n+1) = \lambda x(n) + u(n) - \text{sgn}[x(n)] \qquad (4)$$

is given in [11, 15].

The above presentation demonstrates that high order modulators could be considered as built up of first order modulators, which interact only through the quantizer function. Because of this interaction the stability of the high order SDM depends on the stability of each of the first order modulators, where they have been shifted with respect to the origin of the quantizer function.

To simplify the notations, we will drop the indexes and will rewrite equation (3) in the following form

$$x(n+1) = \lambda x(n) + u(n) - \text{sgn}[bx(n) + y(n)] \qquad (5)$$

where

$$y(n) = \sum_{\substack{i=1 \\ i \neq k}}^{N} b_i x_i(n) \qquad (6)$$

This equation describes a first order shifted system and in what follows we will investigate the stability of this system.

2.2. Stability of shifted first order SDMs

The shifted first order system is described by equation (4). Because of the ideal quantizer, the system can be viewed as two linear systems connected at point $-y(n)/b$ and thus the equations describing the dynamics of the first order SDM from (4) are

$$\begin{aligned} x(n+1) &= \lambda x(n) + [u(n) - 1)], \ x(n) \geq -y(n)/b; \ b > 0 \\ x(n+1) &= \lambda x(n) + [u(n) + 1], \ x(n) < -y(n)/b; \ b > 0 \end{aligned} \qquad (7)$$
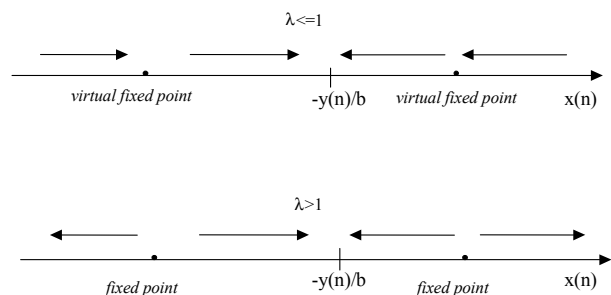
The fixed points of the system are

$$x' = \frac{u(n) - 1}{1 - \lambda}, \quad x'' = \frac{u(n) + 1}{1 - \lambda}$$

In what follows we will consider the input signal $u(n)$ to be from the interval $u(n) \in [-\Delta u, \Delta u]$, $\Delta u > 0$ and because of this the shift $y(n)$ belongs to the interval $[-\Delta y, \Delta y]$, $\Delta y > 0$.

2.2.1. Stable Mode, $\lambda < 1$

The flow diagram of the system is given in Figure 3.

Figure 3. Flow diagrams of the first order system for the case of $\lambda \leq 1$ and $\lambda > 1$.

Depending on the parameters b, $y(n)$ and input signal $u(n)$ the system can have two stable virtual fixed points (the case given in the figure) and a compact region exists between them (in fact this is an invariant set in state space, which has the property that all subsequent states lie in the original set for a certain class of input signals). For another set of parameters one of the virtual fixed points becomes a real fixed point. In each of the cases the system is stable but in the second one, there is no compact region. The system moves towards a single attractor at the stable fixed point. Anyway, if the initial condition is between the origin and the real fixed point

of system (4) the state flow finishes at the equilibrium point (due to asymptotic movement to the single equilibrium point). It should be noted that this is not a desired SDM behavior. The SDM behavior appear when the first order system has two virtual fixed points and the state of (4) jumps between them. Thus the desired bitstream appear at the output of the quantizer. Sufficient conditions for this are object of another research.

2.2.2. Unstable Mode, $\lambda > 1$

The stability in this case is connected with existence of a compact region between the unstable fixed points (not virtual). It is important to point out that b>0. Otherwise the dynamic of the system is described by

$$x(n+1) = \lambda x(n) + [u(n)-1], \; x(n) < -y(n)/b \,; \; b < 0$$
$$x(n+1) = \lambda x(n) + [u(n)+1], \; x(n) \geq -y(n)/b \,; \; b < 0 \quad (8)$$

and it is easy to observe that the above system is always unstable, because at least one of the fixed points is virtual.
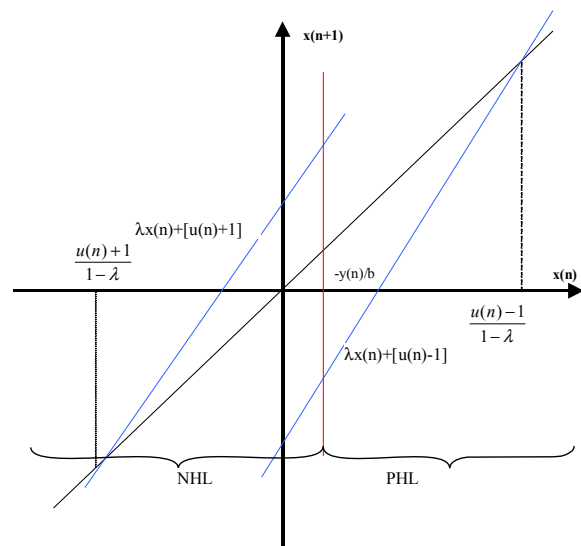

Figure 4. Map (4) given by (7) for the case of $\lambda > 1$

Let's consider the map (4), given by (7) depicted in Figure 4.

For a compact region (CR), to exists the fixed point should not be virtual i.e.

$$-\frac{y(n)}{b} < \frac{u(n)-1}{(1-\lambda)} \;\; \text{and} \;\; -\frac{y(n)}{b} > \frac{u(n)+1}{(1-\lambda)}$$

This should be true for the worst case i.e.

$$-\frac{y(n)}{b} < \frac{\Delta u - 1}{(1-\lambda)} \;\; \text{and} \;\; -\frac{y(n)}{b} > \frac{-\Delta u + 1}{(1-\lambda)}$$

Taking into account that $(1-\lambda) < 0$ and b>0 we get

$$\frac{b}{\lambda - 1}\Delta u - \frac{b}{(\lambda-1)} < y(n) < -\frac{b}{\lambda - 1}\Delta u + \frac{b}{(\lambda-1)} \quad (9)$$

The second condition for the existence of a CR is that the CR has to be included into the region between the fixed points i.e. the stable region (SR). The maximum jump of the variable $x(n)$ from the Negative Half Line (NHL), with respect to $-y(n)/b$, to the Positive Half Line (PHL), with respect to $-y(n)/b$, is $[-y(n)/b]\lambda + [u(n)+1]$ and the maximum jump from PHL to NHL is $[-y(n)/b]\lambda + [u(n)-1]$. Hence in the worst case

$$-\frac{y(n)}{b}\lambda + [\Delta u + 1] < \frac{\Delta u - 1}{(1-\lambda)}$$

$$-\frac{y(n)}{b}\lambda + [-\Delta u - 1] > \frac{-\Delta u + 1}{(1-\lambda)}$$

Solving the above inequalities with respect to $y(n)$ we find that a compact region can only exist if b>0 and

$$b > 0$$

$$\frac{b}{\lambda - 1}\Delta u - \frac{b(2-\lambda)}{\lambda(\lambda - 1)} < y(n) < -\frac{b}{\lambda - 1}\Delta u + \frac{b(2-\lambda)}{\lambda(\lambda - 1)} \quad (10)$$

Because the above should be valid for all y and for $y=0$ as well then $(2-\lambda)/\lambda > 0$ or $\lambda < 2$, i.e. $1 < \lambda < 2$. Due to this $(2-\lambda)/\lambda < 1$ and hence if (10) is satisfied then (9) will be satisfied as well.

Considering again these two conditions, the maximal shift of the input signal Δu, which ensures that the compact region (CR) is included into the region between the fixed points i.e. the stable region (SR) is given by

$$\Delta u < -\frac{\Delta y(\lambda - 1)}{b} + \frac{2 - \lambda}{\lambda} \qquad (11)$$

Note that condition (10) is a sufficient but not necessary condition. It has been derived for the worst case and if satisfied, the first order modulator is stable for the range of input signal given by (11). However, if (10) is not satisfied the modulator could be stable for certain input signal.

2.3. Stability of High Order SDMs with Real Poles

Taking into account the parallel presentation considered in [11, 12], the stability of the high order SDM depends on the stability of each of the first order modulators. If all modes λ_k, are stable, i.e. $\lambda_k<1$ then the corresponding high order SDM is stable in the sense of boundness of the states. If there exists even one unstable mode λ_k, i.e. $1<\lambda_k<2$, the stability conditions for shifted modulators given above should be applied.

In this case the shift $y_k(n)$ depends on the values of the other variables $x_i(n)$ i.e.

$$y_k(n) = \sum_{\substack{i=1 \\ i \neq k}}^{N} b_i x_i(n), \ k = 1,2,...,N \qquad (12)$$

From (10), we have

$$\sum_{\substack{i=1 \\ i \neq k}}^{N} b_i x_i(n) < -\frac{b_k}{\lambda_k - 1}\Delta u + \frac{b_k(2 - \lambda_k)}{\lambda_k(\lambda_k - 1)}$$

$$\sum_{\substack{i=1 \\ i \neq k}}^{N} b_i x_i(n) > \frac{b_k}{\lambda_k - 1}\Delta u - \frac{b_k(2 - \lambda_k)}{\lambda_k(\lambda_k - 1)}, \qquad (13)$$

$$k = 1,2,...,N$$

The above should still be true when x_k makes the maximal "jumps" into the PHL or into the NHL.

Without loss of generality we will consider the first p modes λ_k of the high order SDM to correspond to $1<\lambda_k<2$, $k=1,2,...,p$ whereas the remaining N-p modes correspond to $\lambda_k<1$, $k=p+1,...,N$. In this case only the first p coefficients b_k must be positive and the remaining N-p coefficients could have any real value.

The maximal "jumps" of the state variables corresponding to the first p modes in the PHL and the NHL are $\frac{u(n)-1}{1-\lambda_k}$ and $\frac{u(n)+1}{1-\lambda_k}$, respectively (the fixed points of the system with respect to x_k, $k=1,2,...,p$). Similarly, the maximal "jumps" of the state variables corresponding to the last N-p modes in the PHL and the NHL, are $\frac{u(n)+1}{1-\lambda_k}$ and $\frac{u(n)-1}{1-\lambda_k}$, respectively (the virtual or real fixed points of the system with respect to x_k, $k=p+1,...,N$).

Therefore from (13) for the worst case with respect to the input signal one can obtain

$$\sum_{\substack{i=1 \\ i \neq k}}^{p} b_i \frac{-\Delta u - 1}{1 - \lambda_i} + \sum_{i=p+1}^{N} |b_i| \frac{\Delta u + 1}{1 - \lambda_i} < -\frac{b_k}{\lambda_k - 1}\Delta u + \frac{b_k(2 - \lambda_k)}{\lambda_k(\lambda_k - 1)}$$

$$\sum_{\substack{i=1 \\ i \neq k}}^{p} b_i \frac{\Delta u + 1}{1 - \lambda_i} + \sum_{i=p+1}^{N} |b_i| \frac{-\Delta u - 1}{1 - \lambda_i} > \frac{b_k}{\lambda_k - 1}\Delta u - \frac{b_k(2 - \lambda_k)}{\lambda_k(\lambda_k - 1)}, \qquad (14)$$

$$k = 1,2,..., p$$

Note that we apply (14) only for the shifts connected to the first p modulators. The other N-p first order modulators are stable, because for their corresponding λ_k, $\lambda_k \leq 1$, $k=p+1,...,N$.

If there exists a region $[-\Delta u, \Delta u] \subseteq [-1,1]$, such that $u \in [-\Delta u, \Delta u]$ and for this region conditions (14) are satisfied, then the SDM will be stable for all input signals from this region.

Taking into account equation (14) we get

$$\left[\sum_{i=1}^{p}\frac{b_i}{\lambda_i - 1} - \sum_{i=p+1}^{N}\frac{|b_i|}{\lambda_i - 1}\right]\Delta u < \sum_{i=p+1}^{N}\frac{|b_i|}{\lambda_i - 1} - \sum_{\substack{i=1 \\ i \neq k}}^{p}\frac{b_i}{\lambda_i - 1} + \frac{b_k(2 - \lambda_k)}{\lambda_k(\lambda_k - 1)} \ (15)$$

$$k = 1,2,..., p$$

More detailed considerations of the above inequality shows that in order to ensure a consistent solution of (16) with respect to Δu

$$\sum_{\substack{i=1 \\ i \neq k}}^{p}\frac{b_i}{\lambda_i - 1} - \sum_{i=p+1}^{N}\frac{|b_i|}{\lambda_i - 1} - \frac{b_k(2 - \lambda_k)}{\lambda_k(\lambda_k - 1)} < 0, \quad k = 1,2,..., p \ (16)$$

Hence the maximal shift of input signal Δu ensuring the stability is given by

$$\Delta u < \frac{\sum_{i=p+1}^{N} \frac{|b_i|}{\lambda_i - 1} - \sum_{\substack{i=1 \\ i \neq k}}^{p} \frac{b_i}{\lambda_i - 1} + \frac{b_k(2 - \lambda_k)}{\lambda_k(\lambda_k - 1)}}{\sum_{i=1}^{p} \frac{b_i}{\lambda_i - 1} - \sum_{i=p+1}^{N} \frac{|b_i|}{\lambda_i - 1}}, k = 1, 2, ..., p \ (17)$$

Note that inequalities (17) should be valid simultaneously for each k, $k=1,2,...,p$.

Therefore, together with $b_k>0$, $k=1,2,...,p$, equation (16) gives the *sufficient* conditions for the stability of the SDM, namely

$$\frac{(2 - \lambda_k)}{\lambda_k} \frac{b_k}{(\lambda_k - 1)} > \sum_{\substack{i=1 \\ i \neq k}}^{p} \frac{b_i}{\lambda_i - 1} - \sum_{i=p+1}^{N} \frac{|b_i|}{\lambda_i - 1}, k = 1, 2, ..., p \ (18)$$

For the poles outside the unit circle, $k=1,2,...,p$, we have that $(2-\lambda_k)/\lambda_k<1$. This implies that the inequality, Eq. (18), can only hold for one value of k. Hence, Eq. (18) provides a sufficient condition for stability when $p=1$ i.e. there is at most one unstable mode, and this sufficient condition cannot hold when there is more than one pole outside the unit circle.

It is clear now that in the case of repeated poles ($\lambda_1,...,\lambda_m=\lambda$) of the loop transfer function, the SDM is stable only when the corresponding modes are stable i.e. $\lambda \leq 1$.

Let us consider more precisely the case of identical poles. Without losing the generality we will consider that the pole λ_1 is repeated with order 2 i.e. $\lambda_1=\lambda_2=\lambda$. In this case (2) becomes

$$G(z) = \frac{b_1 z^{-1}}{1 - \lambda z^{-1}} + \frac{b_2 z^{-2}}{(1 - \lambda z^{-1})^2} + ... + \frac{b_N z^{-1}}{1 - \lambda_N z^{-1}} \ (19)$$

And the state equations may be given as

$$x_1(n+1) = \lambda x_1(n) + u(n) - \text{sgn}[b_1 x_1(n) + \sum_{i=2}^{N} b_i x_i(n)]$$
$$x_2(n+1) = x_1(n) + \lambda x_2(n)$$
$$x_k(n+1) = \lambda_k x_k(n) + u(n) - \text{sgn}[b_k x_k(n) + \sum_{\substack{i=1 \\ i \neq k}}^{N} b_i x_i(n)] \quad (20)$$
$$k = 3, ..., N$$

If λ is an unstable mode, *i.e.* $1<\lambda<2$ then the corresponding first and second modulators should be stable in the sense of boundedness of the states. The first one can satisfy the conditions given by (11). The second one in fact is a linear system described by

$$x_2(n+1) = \lambda x_2(n) + x_1(n) \quad (21)$$

where the state variable x_1 could be considered as an input signal for this system. If $1<\lambda<2$ then all possible symbolic sequences represent admissible periodic orbits of x_1. Because of this, depending on the initial conditions a certain periodic orbit of x_1 could influence the instability in x_2.

2.4. Stability of High Order SDMs with Complex Poles

In the general case the loop filter transfer function can have complex conjugated roots. For better understanding, we will present the theoretical solution given in [13], where this case is described in detail. Without loss of generality we will consider only one pair of complex conjugated roots. In this case (2) becomes

$$G(z) = \frac{b_1 z^{-1}}{1 - \lambda_1 z^{-1}} + ... + G_2(z) =$$
$$\frac{b_1 z^{-1}}{1 - \lambda_1 z^{-1}} + ... \frac{B_{N-1} z^{-1} + B_N z^{-2}}{1 - d_1 z^{-1} - d_2 z^{-2}} \quad (22)$$

The denominator of the last part of (22) has a complex conjugated pair of roots. The main idea is to use a complex form of expansion of the last part of $G(z)$. Therefore (22) becomes

$$G(z) = \frac{b_1 z^{-1}}{1 - \lambda_1 z^{-1}} + ... + \frac{b_{N-1} z^{-1}}{1 - \lambda_{N-1} z^{-1}} + \frac{b_N z^{-1}}{1 - \lambda_N z^{-1}} \ (23)$$

where

$$\lambda_{N-1} = \alpha + j\beta, \ \lambda_N = \alpha - j\beta$$
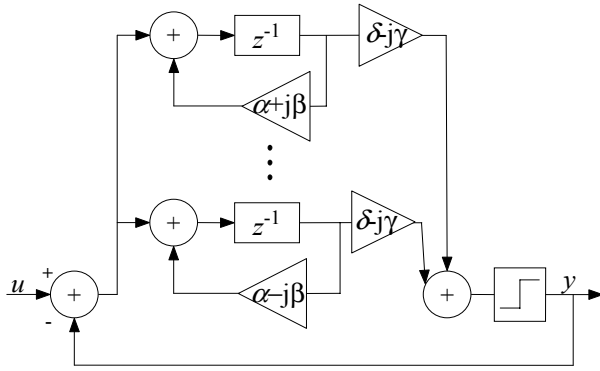$$b_{N-1} = \delta - j\gamma, \ b_N = \delta + j\gamma \quad (24)$$

i.e. λ_{N-1}, λ_N and b_{N-1}, b_N are complex conjugated numbers.

Because of this we can use the same parallel presentation given in figure 2. However, the values of

the last two blocks are complex. It should be stressed that the output signal of these two blocks is real. In order to make things more clear, and without loss of generality we will consider only these blocks. They correspond to a second order SDM with complex conjugated poles of the loop filter transfer function $G(z)$. The block diagram of this modulator is given in figure 5. Here both signals x_1 and x_2 are complex conjugated, namely

$$x_1(k+1) = m(k+1) + jn(k+1)$$
$$x_2(k+1) = m(k+1) - jn(k+1) \qquad (25)$$

Because of this the input of the quantizer is real i.e.

Figure 5. Block diagram of second order modulator with complex conjugate pair of poles.

$$(\delta - j\gamma)x_1(k) + (\delta + j\gamma)x_2(k) = 2\delta m(k) + 2\gamma n(k) \quad (26)$$

As in the case of real poles, the modulator could be considered as two first order modulators interacting only through the quantizer function. The difference now is that the signals connected with both modulators are complex, but the input and output signals (u and y) are the "true" signals of the modulator. This model will help us to make analysis simple. We will consider the state of the first order modulators as a point in a complex plane (m,n). Depending on whether the input $2\delta m + 2\gamma n$ of the quantizer is positive or negative the state equation of the second order modulator could be described as follows:

$$x_1(k+1) = (\alpha + j\beta)x_1(k) + [u(k)-1], 2\delta m(k) + 2\gamma n(k) \geq 0$$
$$x_2(k+1) = (\alpha + j\beta)x_2(k) + [u(k)-1], 2\delta m(k) + 2\gamma n(k) \geq 0 \quad (27)$$

and

$$x_1(k+1) = (\alpha + j\beta)x_1(k) + [u(k)+1], 2\delta m(k) + 2\gamma n(k) < 0$$
$$x_2(k+1) = (\alpha + j\beta)x_2(k) + [u(k)+1], 2\delta m(k) + 2\gamma n(k) < 0 \quad (28)$$

where x_1 and x_2 are given by (26). In fact $2\delta m + 2\gamma n$ is a line through the origin in the plane (m,n) and depending on in what half the point x_1 is (because $x_1 = m + jn$), the description of the modulator is (27) or (28). The analysis of the behavior of both first order "complex" modulators is similar to the analysis of the first order "real" modulators, given in Section 2.2. Here we always should keep in mind that both modulators work cooperative, because their signals are conjugated. These modulators do not exist in the real SDM. They are introduced (like in the "real" case as well) to help us to carry out the analysis of the behavior of the whole system.

2.4.1. Stable Mode, $|\lambda_{N-1}| = |\lambda_N| < 1$

In this case both modulators have two stable equilibrium points (in every half plane):

- first modulator: $\dfrac{u-1}{1-\lambda_1}$ and $\dfrac{u+1}{1-\lambda_1}$ i.e.

$$\frac{(u-1)[(1-\alpha)+j\beta]}{(1-\alpha)^2 + \beta^2} \text{ and } \frac{(u+1)[(1-\alpha)+j\beta]}{(1-\alpha)^2 + \beta^2}$$

- second modulator: $\dfrac{u-1}{1-\lambda_2}$ and $\dfrac{u+1}{1-\lambda_2}$ i.e.

$$\frac{(u-1)[(1-\alpha)-j\beta]}{(1-\alpha)^2 + \beta^2} \text{ and } \frac{(u+1)[(1-\alpha)-j\beta]}{(1-\alpha)^2 + \beta^2}$$

These fixed points could be virtual or real. Taking into account equations (26) to (28), the fixed points of both modulators are "virtual" when $2\delta(1-\alpha) + 2\gamma\beta > 0$ and "non-virtual" when $2\delta(1-\alpha) + 2\gamma\beta < 0$. Both complex modulators are stable and the second order modulator is stable as well. As was mentioned in section 2.2, the SDM behavior appears when the first order system has two virtual fixed points and the states of (28), (29) jump between them. Thus the desired bitstream appears at the output of the quantizer.

According to [13], in the general case, when the last two first order modulators are "complex", i.e. correspond to a stable complex conjugated pair of roots; condition (18) has the form

$$\frac{(2-\lambda_1)}{\lambda_1}\frac{b_1}{(\lambda_1 - 1)} > -\sum_{i=2}^{N-2}\frac{|b_i|}{\lambda_i - 1} + \frac{2|\delta(1-\alpha) + \gamma\beta|}{(1-\alpha)^2 + \beta^2} \quad (29)$$

and the maximal range of input signal Δu ensuring the stability is expressed by

$$\Delta u < \frac{\displaystyle\sum_{i=2}^{N-2}\frac{|b_i|}{\lambda_i-1}-\frac{2|\delta(1-\alpha)+\gamma\beta|}{(1-\alpha)^2+\beta^2}+\frac{b_1(2-\lambda_1)}{\lambda_1(\lambda_1-1)}}{\dfrac{b_1}{\lambda_1-1}-\displaystyle\sum_{i=2}^{N-2}\frac{|b_i|}{\lambda_i-1}+\frac{2|\delta(1-\alpha)+\gamma\beta|}{(1-\alpha)^2+\beta^2}} \quad (30)$$

2.4.2. Unstable Mode, $|\lambda_1|=|\lambda_2|>1$

In this case both modulators have two unstable fixed points (in every half plane). Depending on parameters, these points could be "non-virtual" or "virtual". In the case of virtual fixed points, both "complex" modulators are unstable and the whole system is unstable. In the case of real fixed points, the possibility for SDM behavior is connected with the existence of a compact region in the complex plane. This case is a subject for further research.

2.5. Theory conclusions

To summarise the results on stability of high order SDMs from the previous sections, we have the following;

1. Any SDM comprised entirely of parallel sections with poles inside the unit circle is inherently stable.

2. Any SDM with only real poles is guaranteed to be stable if Eq. 18 holds, and Eq. 17 provides the maximum input for stability. Eq. 18 also implies that the sufficient conditions for stability are violated if at least 2 real poles are outside the unit circle.

3. Any SDM comprised entirely of parallel sections with poles inside the unit circle and one complex conjugate pair inside the unit circle is inherently stable.

4. Any SDM comprised entirely of parallel sections with some real poles outside the unit circle and one complex conjugate pair inside the unit circle is guaranteed to be stable if Eq. 29 holds, and Eq. 30. provides the maximum input for stability. Eq. 18 also implies that the sufficient conditions for stability are violated if at least 2 real poles are outside the unit circle.

It should be emphasized, that present theoretical study includes only the cases considered above; real poles not equal to 1, or complex poles inside the unit circle. It is a subject of further research to cover the cases when the poles are at the unit circle, and the case when a complex pair of poles is outside the circle.

3.   EXPERIMENT

3.1.   Simulation

Within the Matlab environment we have created a sigma delta modulator model using the parallel decomposition technique, according to the theory described in the previous section. The general block diagram of this model has been shown in Fig.2 and Fig.5. In many realistic loop filter designs, there is one first order section with a real pole and the others are grouped into biquad sections. Transforming a second order sections into first order sections results in two first order sections nits with complex conjugate poles, leading to complex signals. For this reason, the experimental implementation, described in Section 3.2, retains the second order sections, whereas the simulation may use the equivalent complex first order sections.

Initially, for performance comparison with existing SDM structures, we ran simulations with the parallel modulator model and the modulator model from the DStoolbox for Matlab[17] using the same loopfilter transfer function on both models. The third order noise transfer function obtained by the DStoolbox, for a 64 times oversampling ratio, was:

$$\text{NTF(z)}=\frac{z^3-2.999z^2+2.999z-1}{z^3-2.1992z^2+1.6876z-0.4441}$$

The relationships between the loop filter, signal transfer function and noise transfer function may be given by[18]:

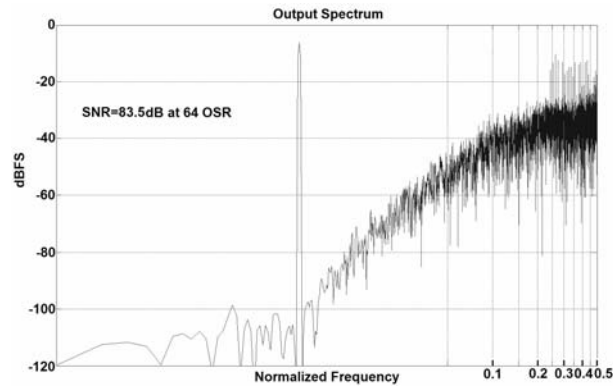$$G(z)=\frac{1}{1-STF(z)}-1=\frac{1}{NTF(z)}-1 \quad (31)$$

which gives the loop filter transfer function:

$$G(z)=\frac{0.7998z^2-1.341424z+0.552171367}{z^3-2.999z^2+2.999z-1} \quad (32)$$

.

Using partial fraction expansion, this may be given in parallel form:

$$G(z) = \frac{10.5599z^{-1}}{1-z^{-1}} + \frac{(-4.8801 - 3.9952i)z^{-1}}{1-(0.9995+0.0316i)z^{-1}} + \frac{(-4.8801 + 3.9952i)z^{-1}}{1-(0.9995-0.0316i)z^{-1}}$$

Simulations confirmed that there was no difference between the parallel and series implementations, with both implementations achieving a signal to noise ration of 83.5db SNR. The power spectrum for both implementations is shown in Fig.6 for an input signal with amplitude 0.5 and frequency 2/3 the bandpass cutoff, 1/64.

Figure 6. Power spectrum of the output signal for an SDM when using the loop filter obtained from (32)

The main advantage of using the parallel decomposition is that it provides us with a means of verifying stability, equations (29) and (30). Thus, using the loop filter transfer function from (32), we then moved the real pole outside the unit circle, while keeping the complex conjugate poles fixed. We then measured the change in the stability range and the change in the SNR as the real pole is moved. The results from these simulations are given in section 4.

Since $G(z)$ has the form of a filter function and we know from equation (31) that we can obtained it from Signal or Noise transfer functions we also started a loopfilter transfer function seeking procedure. We wanted to see how the modulator will behave when using different filter functions for the loopfilter with different cutoff value in order to obtain transfer functions that give us good performance. The cutoff frequency was a scaled value from 0 to 1, where 1 represents $f_s/2$. In this case we had two approaches: one to obtain lowpass filter transfer function that give us STF(z) and the second is

to obtain highpass filter transfer function in order to derive the loopfilter functions from them. We used four filter types – one Butterworth and three Chebyshev type II with 3,6 and 20db stopband ripple. For every model we make a SNR performance measurement, ΔU calculation from (30) and check of condition (29), that guarantees stable operation. The obtained results from this procedure are given in section 4.

3.2. Realisation of high order SDMs with adjustable parameters

When making the PSpice model we had to account for the fact that the circuitry to operated in the *s* domain. For that reason a transformation between $G(z)$ and $G(s)$ is needed. Our third order transfer function with one real pole and a complex conjugate pair of poles may be given as

$$G(z) = \frac{b_1 z^{-1}}{1-\lambda_1 z^{-1}} + \frac{(\delta - j\gamma)z^{-1}}{1-(\alpha + j\beta)z^{-1}} + \frac{(\delta + j\gamma)z^{-1}}{1-(\alpha - j\beta)z^{-1}} =$$
$$= \frac{b_1 z^{-1}}{1-\lambda_1 z^{-1}} + \frac{B_{N-1}z^{-1} + B_N z^{-2}}{1-d_1 z^{-1} - d_2 z^{-2}} \tag{33}$$

Using the bilinear transform:

$$z = \frac{1+sT/2}{1-sT/2} \rightleftarrows p = \frac{2}{T} \cdot \frac{z-1}{z+1} \quad (34)$$

where *T* is the sampling period. For the real pole,

$$G(z) = \frac{b_1 z^{-1}}{1-\lambda_1 z^{-1}} = \frac{b}{z-\lambda} \rightleftarrows$$

$$G(p) = \frac{b}{\dfrac{1+sT/2}{1-sT/2} - \lambda} = \frac{b - sTb/2}{sT/2(1+\lambda)+(1-\lambda)}$$

$$= \frac{\dfrac{b}{1-\lambda} - \dfrac{sTb}{2(1-\lambda)}}{\dfrac{sT(1+\lambda)}{2(1-\lambda)}+1} = \frac{k_1 - k_2 s}{k_3 s + 1} \tag{35}$$

This transfer function is the transfer function of a first order allpass filter. When we substitute the obtained coefficients into the allpass filter structure it has the characteristics of a lowpass filter.

For the complex conjugate pole pair,

$$G(z) = \frac{(\gamma + \delta j)z^{-1}}{1 - (\alpha - \beta j)z^{-1}} + \frac{(\gamma - \delta j)z^{-1}}{1 - (\alpha + \beta j)z^{-1}} =$$

$$= \frac{2\gamma z^{-1} - 2\gamma\alpha z^{-2}}{1 - 2\alpha z^{-1} + (\alpha^2 + \beta^2)z^{-2}}$$

(36)

Again, using the bilinear transform,

$$G(z) = \frac{2\gamma z - 2\gamma\alpha}{z^2 - 2\alpha z + (\alpha^2 + \beta^2)} \rightarrow G(p)$$

$$G(p) = \frac{\left(-\gamma\alpha\left(\frac{T^2}{2}\right) - \gamma\left(\frac{T^2}{2}\right)\right)p^2 + 2\gamma\alpha Tp + 2\gamma(1-\alpha)}{(2\alpha + 1 + \alpha^2 + \beta^2)\left(\frac{T^2}{4}\right)p^2 + (1 - \alpha^2 - \beta^2)Tp + (1 - 2\alpha + \alpha^2 + \beta^2)}$$

$$G(p) = \frac{-\gamma s^2 \frac{T^2}{2}(\alpha + 1) + 2\gamma\alpha Ts + 2\gamma(1-\alpha)}{(2\alpha + 1 + \alpha^2 + \beta^2)s^2 \frac{T^2}{4} + (1 - \alpha^2 - \beta^2)sT + 1 - 2\alpha + \alpha^2 + \beta^2}$$

which is the transfer function of a second order all pass filter. hen substituted with the calculated values like the first order unit has behavior of a lowpass filter.

General form of the schematic of a first order lowpass filter is given in Fig.7, while in Fig.8 the general form of a second order allpass filter is depicted:
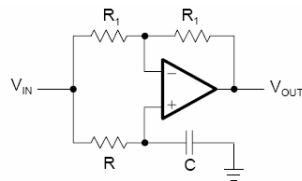

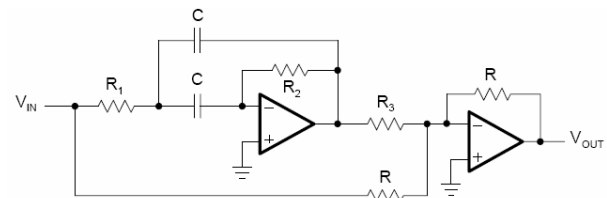
Fig.7 First order allpass filter

Fig.8 Second order allpass filter

In order to set the circuitry according to the G(p) the model consists of a third order SDM with adjustable coefficients. The design employs variable resistors which allow all coefficients within the design to be modified in accordance to the stationary set values of the capacitors. This PSpice design has shown good agreement with the Matlab model at the logic level implementation. Fig.9 depicts the third order modulator PSpice model.

4.   RESULTS

We used a modulator structure with 64 times oversampling ratio for the experiments and simulations. For the case where we have the G(z) obtained by the DStoolbox we have this loopfilter function:

$$G(z) = \frac{0.7998z^2 - 1.341424z + 0.552171367}{z^3 - 2.999z^2 + 2.999z - 1}$$
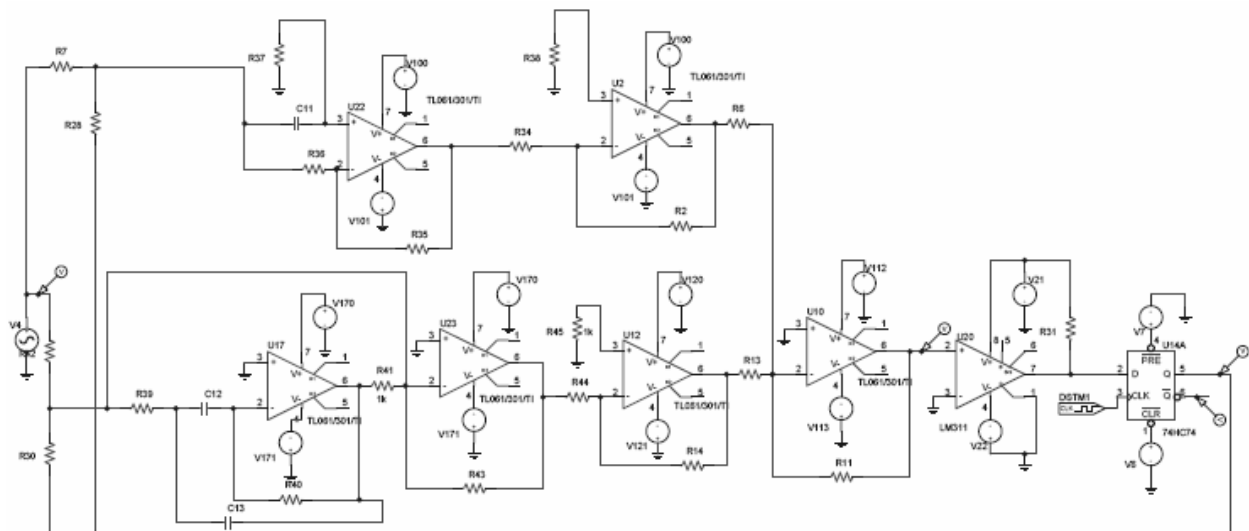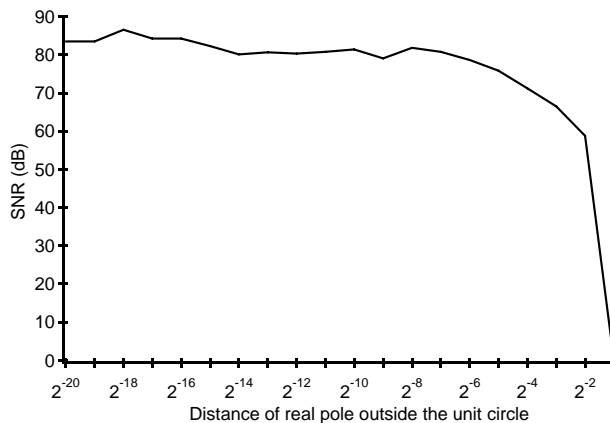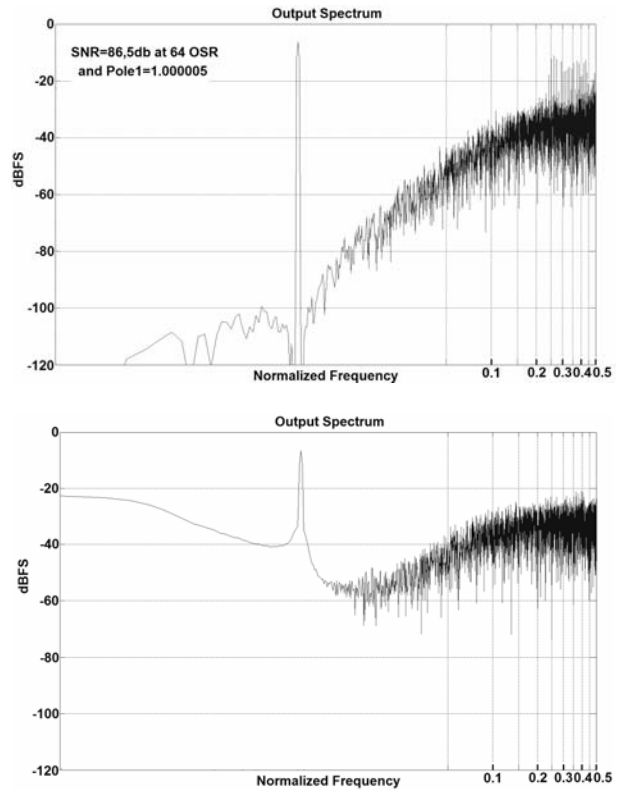

Fig.9 Third order modulator in PSpice

The loopfilter transfer function has the following poles, $p_1=1$, $p_{2,3}=0.9995\pm0.0316i$.

In this specific pole configuration case we can't check Δu, because the present theory does not provide a result when we have a pole lying on the unit circle. However, by moving p_1 inside or outside the unit circle, the theory can be applied. Moving p_1 inside the unit circle leads to severe SNR drop and in this case it is not of interest, because we know that when all the poles are inside the unit circle the modulator will be stable. Moving p_1 slightly outside the unit circle initially leads to a performance increase before the SNR drops.
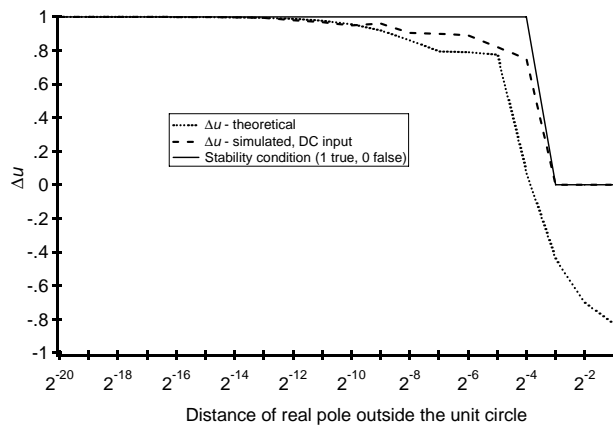

Figure 10. SNR of the SDM given by Eq. (32) when moving the real pole position of the loop filter exponentially outside the unit circle, from $1+2^{-20}$ to 1.5.

Fig. 10 depicts the SNR values obtained when moving the real pole outside the unit circle. The maximum SNR obtained when testing with sine wave as input signal was 86.55 dB, which is higher than the initial function. For all the values of the plotted range up to a real pole position of 1.0625, the stability condition (29) was fulfilled (where we have value of 1 its fulfilled and when we have 0 it is not). The modulator was stable when simulating and testing with DC signals up to almost 1 for all of these cases as the condition (29) and Δu value predicted, despite the fact that we had a pole outside the boundaries of the unit circle.

Figure 11. Plot of the power spectrum when using modified G(z) from (32) with position of the real pole at values 1.000005 and 1.25

When moving the pole further beyond $p_1=1.0625$, the stability check for condition (29) was not fulfilled and when increasing the value of p_1 further, we had a loss of stability. When sinusoidal input was used, the SDM lost its stability at $p_1>1.25$. One quick comparison is shown in Fig. 11 where the power spectrum is shown for two pole position cases. The highest SNR is obtained for $p_1=1.000005$, whereas for $p_1=1.25$ there is a lot of noise in the signal bandwidth and the SNR degrades significantly.

Figure 12. The stability condition, simulated maximum DC input, and theoretical maximum input Δ*u* when moving the real pole position of the loop filter, Eq. (32), exponentially outside the unit circle, from $1+2^{-20}$ to 1.5.
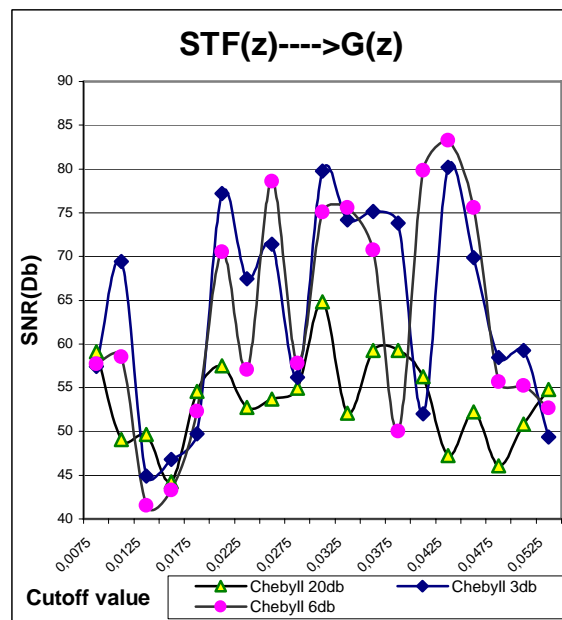
Fig. 12 compares Δ*u*, validity of the stability condition, and maximum stable DC input as the real pole is moved outside the unit circle. By comparing the theoretical sufficient condition for stability with the measured stable range, we have a direct comparison between theory and simulation.

Interestingly, for p_1 between $1+2^{-9}$ and $1+2^{-4}$, stable behavior was observed with larger DC input than predicted by theory. This is most likely because the theoretical condition for stability, in this case Eq. 30, is a sufficient but not necessary condition. Thus, stability may still occur even when this has been violated, as is indeed the case for high DC input and real pole significantly outside the unit circle.

As noted in Section 3, we used 4 filter types with two different approaches to obtain a variety of loop filter transfer functions. The first approach was to find a lowpass filter function which gives the signal transfer functions (STF), and then derive *G*(*z*) using equation (31). SDM performance and stability was then found using this obtained transfer function for the loop filter. We used a cutoff frequency range varying from 0.0075 to 0.0525 by increments of 0.0025 scaled to $f_s/2$. In order to obtain filter transfer function coefficients for filter design software, we used the 'butter' and 'cheby2' Matlab functions that give the filter coefficients for lowpass (STF) or highpass (NTF) Butterworth and Chebyshev II filter designs for specified order and cutoff value. All the third order functions that were

obtained had one real pole and a pair of complex conjugated roots.

Using this approach for the Butterworth filter functions did not provide a sigma delta behavior of the modulator when testing with sine wave input. When testing with DC input in simulations the modulator was stable, but the stability condition (29) was not fulfilled for the whole cutoff test range. Using Chebyshev II filters with 3, 6, or 20db stopband ripple produced modulators which were stable when tested with both sine wave and DC input signal. Fig. 13 provides a combined plot showing the SNR for the different filter types for different cutoff values. For a cut-off frequency of 0.0425, we obtained SNR higher than 80dB on both Chebyshev type II filters with 3 and 6db stopband ripple. The 20db ripple filter provided poor results for the whole range compared with the others and for all filter functions increase of the cutoff value did not produce better results.

Figure 13. SNR versus cutoff performance for STF designed using the Chebyshev II filter.

For all of these transfer functions the Δ*u* value was close to 1, and the modulator was stable in simulations up to 1. Sometimes when the complex pole pair was a little outside the unit circle and the real pole was inside we get a complex value for Δ*u* and condition (29) not fulfilled. For all the cases with higher SNR we have

condition (29) fulfilled and Δu almost equal to 1, which make these transfer functions quite applicable.

The second approach was to find the NTF(z) and then use Eq. (31) to derive the loop filter transfer function. This time with all the filter types in simulations the modulator produced stable behavior for the range depicted in Fig.14.
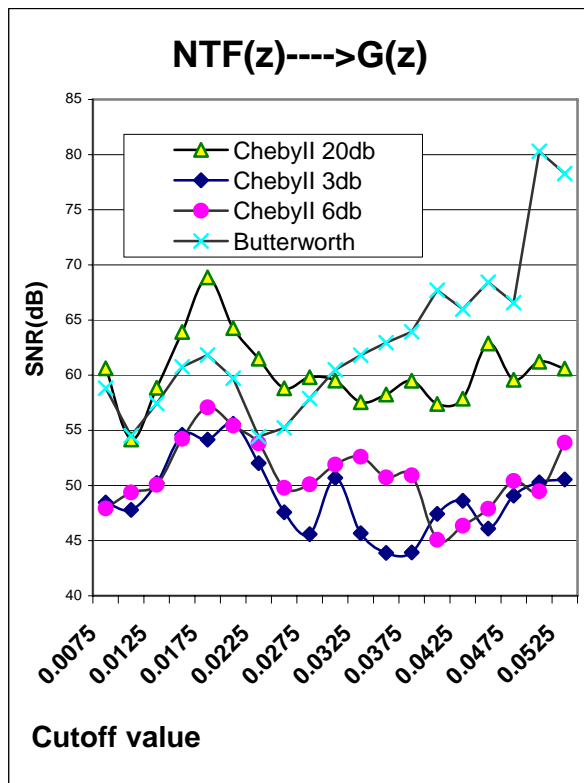

Figure 14.   SNR versus cutoff performance for highpass functions: NTF to $G(z)$ derivation

In contrast with the STF➔$G(z)$ case, and with Butterworth design techniques, we have a definite fulfillment of condition (29) for all the cases considered. We observed that in this case the functions obtained from Chebyshev filters produced lower SNR than when low pass filter design for the STF is used to produce the loop filter transfer function. All these functions with small fluctuations produced Δu around 1, where an example plot for this is show in Fig.15. Despite the fact that condition (29) was not fulfilled for loop filter transfer functions derived from Chebyshev highpass filters, both they and the Butterworth ones were stable when simulating with DC and sinewave test signals. For

the Butterworth filter design increasing the cutoff value lead to a severe drop in the SNR .
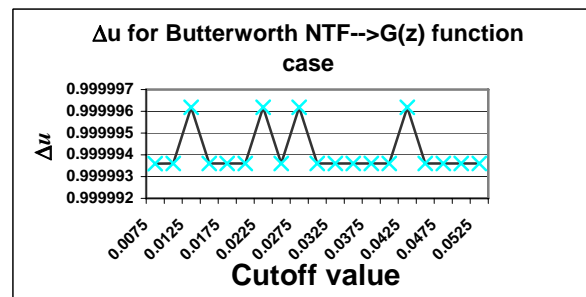

Figure 15. Δu versus cutoff for highpass Butterworth function: NTF to $G(z)$ derivation.
We also observed a strong agreement between the Pspice model and the results obtained with the Matlab model. We observed stable modulator behaviour when using appropriate filter transfer functions. Fig.16 depicts a plot of the SDM input/output signals in the time domain using a sinusoidal test signal.
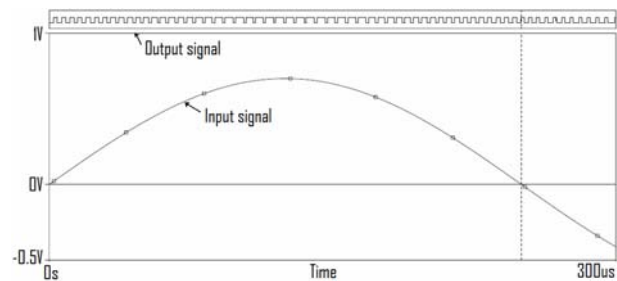

Figure 16. Plot of the sinewave input signal and output bitstream when testing the sigma delta modulator with Pspice.

5.   CONCLUSIONS

In this paper we extend and verify the proposed method for stability analysis of high order SDMs. The method is based on a parallel decomposition of the modulator. The decomposition is presented for both real and complex roots of the denominator of the loop filter transfer function. Using this decomposition the general N^{th} order modulator could be considered as made up of N first order modulators, which interact only through the quantizer function. The decomposition helps us to extract the sufficient conditions for stability of the Nth order modulator. They are determined by the stability conditions of each of the first order modulators but shifted with respect to the origin of the quantizer

function, because of the influence of all other first order modulators. The results have been confirmed by both theory and simulation.

The results presented here represent a work in progress. As of this writing, the experimental system has been constructed and tested. It produces the expected sigma delta modulator behavior, but it remains to be seen if it will produce similar stability results as were found from theory and simulation. Furthermore, the theory needs to be extended to more cases, such as poles on the unit circle, repeated complex poles, or complex poles outside the unit circle.

6.   ACKNOWLEDGEMENTS

7.   REFERENCES

[1]R. Farrell and O. Feely, "Bounding the integrator outputs of second order sigma-delta modulators," *IEEE Trans. Circuits and Systems, Part II: Analog and Digital Signal Processing,* vol. 45, pp. 691-702, 1998.

[2]L. Risbo, "Sigma-Delta Modulators - Stability Analysis and Optimization," PhD Thesis, *Electronics Institute.* Lyngby: Technical University of Denmark, 1994, pp. 179. http://eivind.imm.dtu.dk/publications/phdthesis.html

[3]R. Schreier, M. Goodson, and B. Zhang, "An algorithm for computing convex positively invariant sets for delta-sigma modulators," *IEEE Trans. Circuits and Systems I: Fundamental Theory and Applications*, v. 44, pp. 38-44, 1997.

[4]B. Zhang, M. Goodson, and R. Schreier, "Invariant Sets for General Second-Order Lowpaws Delta-Sigma Modulators with DC Inputs," ISCAS, pp. 1-4, 1994.

[5]M. Goodson, B. Zhang, and R. Schreier, "Proving Stability of Delta-Sigma Modulator Using Invariant Sets," ISCAS, pp. 633-636, 1995.

[6]S. Hein and A. Zakhor, "On the stability of sigma-delta modulators," *IEEE Trans. Signal Processing*, vol. 41, pp. 2322–2348, 1993.

[7]H. Wang, "On the Stability of Third-Order Sigma-Delta Modulation," ISCAS, Chicago, Illinois, p. 1377-1380, 1993.

[8]J. Zhang, P. V. Brennan, D. Jiang, E. Vinogradova, and P. D. Smith, "Stable boundaries of a third-order sigma-delta modulator," Southwest Symposium on Mixed-Signal Design, pp. 259 - 262, 2003.

[9]J. Zhang, P. V. Brennan, D. Jiang, E. Vinogradova, and P. D. Smith, "Stability analysis of a sigma delta modulator," International Symposium on Circuits and Systems ISCAS, pp. I-961 - I-964, 2003.

[10]J. Zhang, P. V. Brennan, P. D. Smith, and E. Vinogradova, "Bounding attraction areas of a third-order sigma-delta modulator," International Conference on Communications, Circuits and Systems, ICCCAS, pp. 1377 - 1381, 2004.

[11]P. Steiner and W. Yang, "Stability of high order sigma-delta modulators," 1996 IEEE International Symposium on Circuits and Systems, ISCAS '96, pp. 52 - 55, 1996.

[12]P. Steiner and W. Yang, "A framework for analysis of high-order sigma-delta modulators," *IEEE Trans. Circ. and Systems II: Analog and Digital Signal Processing*, p1-10, 1997.

[13]V. Mladenov, H. Hegt, and A. v. Roermund, "On the Stability Analysis of Sigma-Delta Modulators," 16th European Conference on Circuit Theory and Design ECCTD 2003, Cracow, Poland, pp. I-97 - I-100, 2003.

[14]V. Mladenov, H. Hegt, and A. Roermund, "On the Stability Analysis of High Order Sigma-Delta Modulators," *Analog Integrated Circuits and Signal Processing*, v. 36, 2003.

[15]V. Mladenov, H. Hegt, and A. v. Roermund, "Stability Analysis of High Order Sigma-Delta Modulators," 15th European Conference on Circuit Theory and Design ECCTD, Helsinki, Finland, pp. I-313 - I-316, 2001.

[16]V. Mladenov, H. Hegt, and A. v. Roermund, "On the Stability of High Order Sigma-Delta Modulators," 8th IEEE International Conference on Electronics, Circuits and Systems ICECS, Malta, pp. 1383 - 1386, 2001.

[17]R. Schreier and G. C. Temes, *Understanding Delta-Sigma Data Converters*. New Jersey: John Wilet & Sons, 2005.

[18]J. D. Reiss, "Understanding sigma delta modulation: the solved and unsolved issues," *Journal of the Audio Engineering Society*, vol. 56, pp. 49-64, 2008.